State of Florida Hurricane Loss Projection Model: Atmospheric Science Component

Mark Powell[a*], Steve Cocke[b],George Soukup[a], Sneh Gulati[c],
Nirva Morisseau-Leroy[d], Chris Landsea[a], Neal Dorst[a] and Liza Axe[b]

[a]NOAA Hurricane Research Division, Miami FL USA

[b]Florida State University, Tallahassee, FL USA

[c]Florida International University, Miami FL USA

[d]University of Miami, Miami, FL USA

Abstract

The State of Florida is in the process of developing an open, public model for the purpose of probabilistic assessment of risk to insured residential property associated with wind damage from hurricanes. The model comprises atmospheric science, engineering, and financial/actuarial components and is planned for 2004 submission to the Florida Commission on Hurricane Loss Projection Methodology. The atmospheric component includes modeling the track and intensity life cycle of each simulated hurricane within the Florida threat area. When a storm approaches within 200 km of the Florida coast line, the wind field is computed by a slab model of the hurricane boundary layer coupled with a surface layer model based on the results of recent GPS sonde research. A time series of open terrain surface winds is then computed for each zip code in the threatened area. Depending on wind direction, an effective roughness length is assigned to each zip code based on the upstream roughness as determined from land cover/ land use products. Thousands of storms are simulated allowing determination of the wind risk for all zip codes in Florida. The wind risk information is then provided to the engineering and loss models to assess damage and average annual loss, respectively.

Keywords: Hurricane, risk, loss, catastrophe

1. Introduction

The historical record for establishing the risk of hurricanes throughout the coastal United States is limited to a period of about 100 years. Unfortunately this period is not sufficient to establish risk without large errors so alternative methods have been used since the 1970's (Ref [1]). Hurricane risk models are currently used to conduct simulations of thousands of years of storms based on statistical probability distributions of important historically observed parameters. This method is often referred to as the joint probability method since the probability of having an event is coupled with the probability that the event is of a given intensity. Commercial modeling interests have developed several versions of these which are used to advise the insurance industry for ratemaking. Unfortunately the models are proprietary so customers whose rates have increased on the basis of model calculations have no way of of examining or questioning the

results. The State of Florida is developing a public model to provide an understandable baseline for comparison to the commercial models. The model will be open and transparent, in which results can be examined in great detail. This paper will describe the atmospheric component of the model.

2. Threat area

To focus on storms capable of causing residential property damage in Florida, a threat area is defined to best capture the statistical characteristics of historical tropical cyclones that have affected the state. The area within 1000 km of a location (26.0 N, 82.0W) off the southwest coast of Florida (Fig. 1) was chosen since this captures storms that can affect the panhandle and northeast coasts of Florida, as well as storms that approach South Florida from the vicinity of Cuba and the Bahamas.

3. Annual occurrence and storm genesis

The model has the capability of simulating climate cycles and tropical cyclone activity according to different periods of the historical record (Ref[2]). The period 1851-2002 is the latest available but the period 1900-2002 is frequently used due to uncertainties about 19th century storms, especially for Florida. There are also uncertainties about the first half of the 20th century since aircraft reconnaissance only began in the 1940's so another choice in the period of record is the period 1944-2002. Four additional choices are available which simulate the warm (El Nino, fewer hurricanes) and neutral or cold (La Nina, more hurricanes) inter annual climate cycles in tropical cyclone activity, as well as the cold or warm phases of the Multi-decadal climate cycles. These choices constrain the historical record from which the fit of annual tropical cyclone occurrence is made. Two fits are tested, the negative binomial and the Poisson model. Goodness of fit tests determine which fit is used for the subsequent simulations. Once the number of tropical cyclones within the threat area for a given year is determined, the historical seasonal genesis frequency is empirically fit to determine the date and time of genesis for each storm.

4. Storm movement and intensity

The threat area is divided which into regions which contain the historical and seasonal characteristics of storm motion and intensity change. Initial location, intensity, and motion for each storm are based on the geographic probability distributions of each quantity for a given time within the season. We use a stochastic approach to model the storm genesis location and track and intensity evolution. A PDF for the initial storm position is derived from the historical "genesis" data, where by genesis we mean the time when the storm forms in or first appears in the threat area. The PDF is a derived for 0.5 degree latitude/longitude box regions, as well as time of season (month). A (uniform) random error term is added so that the storm may form anywhere within the 0.5 degree box. Figure 2 shows a plot of the spatial PDF for storm genesis location for the month of August.

We derive discrete PDFs based on historical data to provide the initial and subsequent motion and intensity of the storm. A storm is simulated by repeatedly sampling from these PDFs via a Monte Carlo approach. These PDFs are derived for variable-sized regions centered at every 0.5 degree latitude and longitude in the hurricane basin. The size of these regions is determined to be that which gives a robust probability density function (PDF) for the quantities of interest (speed, direction, and intensity), up to some maximum size. Once the storm has been given an initial condition, its subsequent evolution is governed by sampling the PDFs for change in intensity, change in translation speed, and change in heading angle in 6 hour increments. The time step is reduced to 1 hour when the storm is close to the coastline.

Intensity change is modeled by using the observed geographic probability distribution of six-hour changes of central pressure through modeling the potential intensity (Ref [3]). The potential intensity takes into account the concept of the hurricane as a heat engine constrained by the input (sea surface) and outflow (stratosphere) temperatures. Intensity change is limited so as to not exceed the maximum observed change for a particular geographic region. When a storm center crosses the coastline (landfall) the intensity change follows a pressure decay model (discussed below). If the storm moves back over the sea, the former intensity change model is reinstated.

The PDFs for change in speed and direction depend on the current speed and direction (binned in discrete intervals), as well as geographic location (0.5 degree lat-lon location) and time of season (month). Figure 3 shows a PDF for change in direction for 8 possible direction intervals (45 degree intervals). The PDF indicates that the storm has a high probability for maintaining current direction, except for westward traveling storms which tend to turn right (northward) somewhat.

This approach has a great advantage over early models that considered a circular approach region surrounding coastal cities. Storms that parallel the coast or make several landfalls can be properly simulated with this method.

5. Storm decay

The tropical ocean is typically warmer than the air above it, enabling a transfer of heat and moisture to the air. Inflow towards the center of the tropical cyclone transports this energy toward the eyewall, where it can help sustain convection, leading to a positive feedback of warming in the eye, lower minimum central pressure, stronger inflow, and more energy transport (Ref [4], [5]). Over the ocean this positive feedback loop may be slowed or reversed by ocean cooling, advection of relatively cold dry air with a history of travel over land, or strong wind shear that prevents the storm center from focusing heating in the eye (Refs. [6], [7]). As a hurricane make landfall, more and more of the circulation traverses land, and the storm loses it's source of energy (Ref. [8]). More and more dry and relatively cool air flows towards the center, and the air cools even more as it expands adiabatically while approaching lower pressures (Ref. [9]). The result is that the eye heating gradually decreases and the central pressure begins to increase or "fill".

Since the wind model depends on the specification of the pressure gradient, a method was needed to estimate the central pressure over land. The central pressure is modeled using the filling model of Vickery and Twisdale [10].

The HURDAT database and Ho et al. [11] contains documentation of storm decay and pressure filling for many hurricane landfall cases in the historical record. As a starting point for a simple decay model we will use the exponential decay as a function of time after landfall. Vickery and Twisdale [10] developed and tested a model for the Florida peninsula based on nine landfalling hurricanes and found the model to be slightly conservative within 3 h of landfall and slightly non conservative beyond 3 h after landfall. The form of the model is:

$$\Delta p(t) = \Delta p_0 \exp(-at) \qquad (1)$$

where $\Delta p(t)$ is the time dependent central pressure deficit and t represents the time after landfall. The filling rate constant is given as:

$$a = a_o + a_1 \Delta p_o + \varepsilon \qquad (2)$$

where ε is a random error term with a normal distribution. The dependence of the filling rate constant on Δp allows stronger storms to decay faster than weak storms; a characteristic observed in hurricane landfalls (Ref. [12]). The random error term allows for the possibility that some storms will decay slower or faster than average. For the Florida peninsula Vickery and Twisdale (1995) use a_o=0.006, a_1= 0.00046, and the standard deviation of ε = 0.0025.

The Kaplan and DeMaria [13] model is also pertinent but it deals with wind decay rather than pressure decay and there is no well established method to convert inland-decayed peak winds to central pressure. The advantage of the filling model is that it provides a starting point to invoke an intensity redevelopment for storms that exit the coastline and reintensify over water. When a storm reemerges over water, the intensity is modeled along the track the same way it was before landfall using the decayed pressure as an initial value.

6. Wind field model

Once a simulated hurricane moves to within 200 km of the Florida coastline, the wind field model is turned on. The model is based on the slab boundary layer concept originally conceived by Ooyama [14] and implemented by Shapiro [15]. Similar models based on this concept have been developed by Thompson and Cardone [16] and Vickery et al. [16, 17]. As in Ref. [15] the model is initialized by a vortex in gradient balance with the pressure above the boundary layer. Gradient balance represents a circular flow caused by balance of forces on the flow whereby the inward directed pressure gradient force is balanced by an outward directed Coriolis and centripetal accelerations. The coordinate system translates with the hurricane vortex moving at velocity **c**. The vortex translation is assumed to equal the geostrophic flow associated with the large scale pressure gradient. As a possible future enhancement the large scale flow in which the vortex is embedded may be treated independently of the vortex motion as in Ref. [16]. In cylindrical coordinates that translate with the moving vortex, equations for a slab hurricane boundary layer under a prescribed pressure gradient (Ref. [15]} are:

$$\frac{u\partial u}{\partial r} - \frac{v^2}{r} - fv + \frac{v}{r}\frac{\partial u}{\partial \theta} + \frac{\partial p}{\partial r} - K\left(\nabla^2 u - \frac{u}{r^2} - \frac{2}{r^2}\frac{\partial u}{\partial \theta}\right) + F(\vec{c},u) = 0 = \frac{\partial v}{\partial t} \quad (3)$$

$$u\left(\frac{\partial v}{\partial r} + \frac{v}{r}\right) + fu + \frac{v}{r}\frac{\partial v}{\partial \theta} - K\left(\nabla^2 v - \frac{v}{r^2} + \frac{2}{r^2}\frac{\partial u}{\partial \theta}\right) + F(\vec{c},v) = 0 = \frac{\partial u}{\partial t} \quad (4)$$

where u and v are the respective radial and tangential wind components relative to the moving storm, p is pressure which varies with radius (r), f is the Coriolis parameter which varies with latitude, θ is the azimuthal coordinate, K is the eddy diffusion coefficient, and F(c,u), F(c,v) are frictional drag terms (discussed below). All terms are assumed to be representative of means through the boundary layer. The motion of the vortex is determined by the modeled storm track.

Note that equations (3) and (4) represent a steady state solution. In order to solve the equations they must be integrated until the steady state assumption is satisfied either through time integration (e.g. Ref. [16]) or numerical method (see model integration section below and appendix). More sophisticated multiple level models (e. g. Kurihara et al., [19]) include equations describing the thermodynamic processes including convection, cloud and precipitation microphysics, evaporation of sea spray, exchange of heat and moisture with the sea, etc. These processes interact to change the pressure and wind fields over time, but the computational requirements of such models make them poorly suited for risk assessment. An advantage of our approach is that the solution to (3) and (4) is straightforward and we do not have the computationally costly requirement to run the model to "steady state" each time we desire a solution. A limitation of our model (and all other Hurricane risk models) is the lack of physical representation of processes that may also contribute to the wind field of a tropical cyclone.

6.1 *Surface pressure field*

The symmetric pressure field p(r) is specified as:

$$p(r) = p_o + \Delta p e^{-\left(\frac{R_{\max}}{r}\right)^B} \quad (5)$$

where p_o is the central minimum sea level pressure, *B* is the Holland [20] pressure profile shape parameter, Rmax is the radius of maximum gradient wind speed, and Δp is the pressure deficit or difference between p_o and the peripheral pressure at the location of the outermost curved pressure contour on a surface synoptic weather map. The central pressure is modeled according to the intensity modeling in concert with the storm track. The peripheral pressure is held constant at 1013 kPa in accordance with the mean global atmospheric surface pressure.

The mean tangential gradient wind is determined primarily by (5). In the development of the

HAZUS model for FEMA, the contractor demonstrated that the azimuthal location and radial extent of peak winds is very sensitive to *B*. Vickery et al. [18] used a NOAA-HRD database of research and reconnaissance aircraft measurements to study the dependence of *B* on po and Rmax observed by the aircraft at altitudes < 1.5 km, which Dunion et al. [21] have shown are representative of the mean boundary layer. The resulting Ref. [18] expression for B is:

$$B = 1.38 + 0.00184\Delta p - 0.00309 R_{\max} \qquad (6)$$

Expression (6) is used at present but a new method of pressure profile specification is under development by Willoughby [22].

6.2 *Radius of maximum wind*

The radius of maximum wind is determined from a distribution of values as a function of Pmin and latitude. As in Ref. [18], a log normal distribution is assumed for Rmax with a mean value determined as a function of ∆p and Latitude. In developing the models for Rmax, we used the data from Ref. [11] for storms from 1900-1983, NOAA-HRD archives of realtime surface wind analyses from 1995-2002, an archive of the National Hurricane Center that was maintained by Dr. Mark DeMaria (now with NOAA's NESDIS at Colorado State University) for the years 1988-1999, and an HRD archive of aircraft observations for the years 1984-1987. The State of Florida model considers U. S. Atlantic coast hurricane landfalls with latitudes as high as 34 degrees north in order to help fill a dearth of information on storms affecting the Northeast Florida coastline. A generalized linear model for the natural log of Rmax ($r^2 = 0.212$) is

$$\ln R_{\max} = 2.0633 + 0.0182\Delta p - 0.00019008\Delta p^2 + 0.0007336 Lat^2 + \varepsilon \qquad (7)$$

where ε is a normal random variable with a mean of zero and a variance of 0.169. Equation (7) describes the mean of the log normal distribution in nm. When a simulated storm is close enough to land to become a threat, an Rmax value is randomly chosen given the ∆p and Latitude.

6.3 *Friction terms*

The frictional drag is in the direction opposite the total wind relative to the earth at the surface and represents the mean momentum flux from the atmosphere to the surface. The frictional terms in (3) and (4) may be specified in terms of the vertical gradient of stress:

$$F(\vec{c}, u) = \frac{\partial \tau}{\partial z} \qquad (8)$$

The variation of τ with height over the depth of the slab boundary layer may be described by a function with properties supported by observations in the surface layer of tropical cyclones. Here we invoke the concept of a surface layer as the lower region of the boundary layer estimated at 200m in which stress is approximately constant. In reality the stress is greatest close to the surface, and is zero at the top of the boundary layer. By assuming stress as near constant over the surface layer we satisfy conditions for applying the logarithmic wind profile to describe the

vertical variation of the mean wind speed with height. The fact that a mean logarithmic wind profile has been observed in tropical cyclone eyewalls (Ref. [23]) provides justification for the surface layer concept. The evaluation of (8) may be approximated as 0.25 (τ_{sfc} / h), where τ_{sfc} is the surface stress and h represents the top of the boundary layer, taken to be 500 m. The factor 0.25 takes into account the fact that the average stress in the slab boundary layer is less than the mean stress of the surface layer. The 0.25 value is an estimate based on meteorological judgment. At the surface, the stress may be expressed in terms of the earth relative surface wind velocity U10 at a height of 10 m or 32 ft above the surface, and the neutral stability surface drag coefficient, Cd :

$$\tau_{sfc} = Cd\left|\vec{U}_{10} + \vec{c}\right|\left(\vec{U}_{10} + \vec{c}\right) \qquad (9)$$

where

$$C_d = \left(0.49 + 0.065\left|\vec{U}_{10} + \vec{c}\right|\right)x10^{-3} \qquad (10)$$

as specified by Large and Pond [24] and U_{10} is the surface (10 m, 32 ft) wind speed relative to the moving storm. Recent research by Powell et al., [23] has indicated that (10) may not apply in the open ocean but at present we believe it is appropriate near the coast where shoaling conditions would be expected and where the wind model is applied to assess risk.

As described below, U_{10} may be expressed in terms of the mean boundary layer wind, as supported by recent GPS sonde measurements in hurricanes:

$$\left|\vec{U}_{10}\right| \approx 0.8\left|\vec{u}\right| \qquad (11)$$

6.4 *Eddy Diffusion*

The wind model describes the effects of horizontal turbulence following Shapiro [15] using a constant eddy diffusion coefficient, k = 5 x 10^4 m^2s^{-1}. In theory the role of eddy diffusion is to represent the effect of turbulence in mixing air horizontally in the radial and tangential directions. Vertical mixing (contained in the friction terms discussed earlier) is typically much larger in magnitude and is associated with a large body of research based on numerous field investigations. Horizontal mixing is most prominent in regions with strong horizontal gradients. Hence the greatest impact of eddy mixing will be in the eyewall where radial gradients are strong. In practice, this term primarily serves as a way to smooth out computational noise in the model results.

6.5 *Model integration*

The Hurricane wind field model includes a fully two dimensional, time-independent, numerical integration of the tangential and radial momentum equations for the mean boundary layer wind components (see Appendix for a complete description). The actual integration procedure is an iterative one, which makes use of a polar coordinate integration grid (Fig. 4) centered on the moving storm. The nested circles are separated from their inscribed and circumscribed neighbors by a radial separation of $R_{max}/10$, where R_{max} is the prescribed radius of maximum winds.

The integration proceeds in two separate but interlocking steps: The "ring" integration treats each concentric ring of grid points as if the radial derivatives in the momentum equations for the tangential and radial wind components are precisely known. Hence, the "ring" equations determine the tangential and radial wind components at each grid point on one of the concentric rings by solving two nonlinear coupled ordinary differential equations in the azimuthal variable with periodic boundary conditions. This integration is performed on each one of the concentric rings covering the domain of integration out to a distance of 20 R_{max}. The "spoke" integration treats each radial spoke of grid points as if the azimuthal derivatives are precisely known. Therefore, the "spoke" equations determine the tangential and radial wind components at each grid point on one of the "spokes" emanating outward from the origin by solving two coupled nonlinear ordinary differential equations in the radial variable measured in units of the RMW.

Since the "ring" process needs radial derivatives and the "spoke" process requires azimuthal derivatives, both of these processes can be started simultaneously by computing the requisite radial derivatives from an initial approximate wind field, which is computed for a stationary storm, and setting the azimuthal derivatives to zero. The asymmetry in the final wind field arises primarily from the fact that the friction terms are both proportional to the term:

$$\left|\vec{W}\right|\vec{W} - |\vec{c}|\vec{c} = \left|\vec{V} + \vec{c}\right|\left(\vec{V} + \vec{c}\right) - |\vec{c}|\vec{c} \qquad (12)$$

where $\vec{W}$ is the earth-relative total vector wind, $\vec{V}$ is the storm-relative total vector wind and $\vec{c}$ is the constant translational velocity. Thus, the asymmetry in the final result arises explicitly through the dependence on $\vec{c}$ as well as implicitly through induced asymmetry in $\vec{V}$. At the outset of the iteration, $\vec{V}$ has no azimuthal dependence since it was computed for a stationary storm. Hence the results of the first iteration yield "ring" and "spoke" wind fields (Fig. 5) which exhibit asymmetry solely due to the explicit dependence of the friction terms on the translation velocity. The friction terms computed from the initial wind field are used to provide the "given" terms in both the "ring" and spoke" equations which, separately, upon integration, furnish an improved version of the complete vector wind field, which is asymmetric. An optimum linear combination of the "ring" and "spoke" wind fields is then determined to

minimize the residuals of the complete set of fully two dimensional momentum equations. This optimum mixture of the "ring" and "spoke" wind fields, which is asymmetric, replaces the initial storm-relative wind field and the integration cycle can be repeated as often as needed. After a few iterations, the process converges such that there is very little difference between the "ring" and "spoke" wind fields or successive instances of the optimized composite wind field. The latest instance of the composite wind field (Fig. 6) is the model solution for the wind components in the translating coordinate system. A simple coordinate transformation then produces the earth-relative wind field based on the known translation velocity. Our methodology directly determines a "steady state" wind field describing a uniformly translating cyclone moving over a uniform surface with given frictional characteristics.

6.6 *Asymmetries in the wind field*

The solution of (3) and (4) exhibits a shift of the radius of maximum winds toward the center when compared with the gradient wind profile. The tangential winds are also super gradient due to the advection inward of angular momentum due to the radial flow induced by the frictional convergence. Besides vortex translation motion, radial advection of tangential momentum, and differential friction, other factors affecting the asymmetric distribution of winds in a tropical cyclone include wind shear, synoptic scale weather features, rainband convection, concentric eyewall cycles, and tertiary circulations associated organized linear flow features and turbulent eddies. In the simple model described here, only the motion and differential friction influences are taken into account. The remaining features are difficult to model but play an important role in determining the azimuthal location of the peak wind. A future version of the model will attempt to include the effects of wind shear.

6.7 *Marine surface layer*

Once the mean PBL motion field is determined, the surface wind is estimated through surface layer modeling. A neutral stability surface layer is assumed to exist. Monin-Obukov heights provide an estimate of the importance of shear or mechanically produced turbulence to buoyancy-produced turbulence. The large values of Monin-Obukov heights computed in tropical cyclones by Moss and Rosenthal [25] and Powell [26] are consistent with shear induced turbulence associated with neutral, well-mixed surface layers. In these conditions we can specify the surface stress and friction velocity in terms of a drag coefficient, and use the well known log profile to describe the variation of wind speed with height. The mean boundary layer (MBL) depth is assumed to be 500 m, and the MBL wind speed is assumed to apply to the midpoint of this layer or 250m. A log profile for neutral stability is assumed to apply from the surface (10 m) to 250 m. Recent research on marine boundary layer wind profiles in tropical cyclones (Ref. [23]) support this assumption. The mean surface wind for marine exposure is assumed to be 78% of the slab boundary layer wind, in accordance with recent results from over 300 boundary layer wind profiles observed in tropical cyclones (Ref. [23]). The height and exposure of the model surface wind is 10 m and "open" in accordance with standard ASTM 1996 and is assumed to represent a mean over a 3600 s time period. A gust factor (Ref. [27]) is used to

convert the mean wind to a maximum sustained one min wind as required by the State of Florida Commission on Hurricane Loss Projection, and to a peak 3s gust as required for the engineering component damage calculations. An example of the model wind field for Hurricane Andrew compared to a published observation-based wind field (Ref. [6]) is shown in Fig. 6.

Considering the wind shears present in tropical cyclones and the lack of cold sea surface temperatures in the vicinity of the Florida coastline, the neutral boundary layer assumption is justified. The marine roughness is modeled using the Large and Pond [24] drag coefficient to compute friction velocity given the mean surface wind speed, and then solving the neutral stability log law for for Zo. The Ref. [24] expression for drag coefficient was found to compare well with open ocean measurements in hurricanes for wind speeds up to hurricane force. For higher wind speeds, recent hurricane measurements (Ref. 23) suggest that the drag coefficient and roughness decrease with wind speed over the open ocean. However, since the use of the hurricane model for loss projection will apply to the landfall of the tropical cyclone where conditions are very different than those over the open ocean. Anctil and Donelan [28] suggest that shoaling conditions in the shallow water adjacent to the coastline cause increased roughness and drag coefficient. The Large and Pond expression dependence on wind speed estimates larger values that we assume are relevant to shoaling conditions. Sufficient measurements to improve the modeling of drag and roughness near the coast will not be available for several more years.

7. Land friction influences

To standardize observations for a common terrain (Ref. [27]), the mean surface wind for marine conditions is converted to "open terrain" conditions over land using the expression given in Simiu and Scanlan [29]. For each 10 min segment of storm motion, the open terrain exposure surface wind speed and direction is determined for all population-weighted zip code centroid locations within 200 km of the storm center. The open terrain wind at each zip code centroid is corrected to the observed terrain using a fetch-dependent virtual roughness for that particular direction and zip code. The virtual roughness takes into account the flow over upstream changes in roughness and assumes that internal boundary layer development prevents the flow from reaching complete equilibrium with its surroundings (Refs. [27, 30]). The flow is most influenced by the roughness of the terrain 3 km upstream of the zip code centroid, but the flow is still influenced by terrain further upstream. The approach we use is based on the Source Area Model (SAM) described in Schmidt and Oke [31]. SAM takes into account turbulence created by patchy terrain and determines the relative importance of the turbulence source area to a downstream wind sensor located at the zip code centroid. This approach is an improvement over current models that consider zip code roughness constant for all wind directions. Our method is especially advantageous for coastal zip code locations since flow with an upstream fetch over the sea can be significantly stronger than flow over a constant land roughness. The geographic distribution of roughness (Fig. 7) is associated with a classification of the land use / land cover in a particular region according to LANDSAT imagery used to develop the National Multi-Resolution Land Cover database (Ref. [32]). Determination of the roughness for each LU/LC classification was developed by the National Institute for Building Sciences for FEMA's multi

hazard damage mitigation model (HAZUS).

The maximum sustained 1 min surface wind and peak 3 s gust are computed by applying a gust factor (Ref. [27]) to the the mean surface wind. At the end of a simulation, time series of wind speed and direction exist for all zip codes in Florida for which hurricanes (or hurricanes that have decayed to a weaker status) have passed within 200 km. Landfalling tropical storms and hurricanes that have decayed post-landfall to a tropical storm with maximum winds of <18 m/s are are not considered. The great advantage of our approach over other models is that the full time series of the wind are retained at high resolution. Retaining this information makes possible the determination of additional damage-relevant parameters such as duration of winds exceeding hurricane force and wind steadiness. Powell et al [33] showed that damage to the building envelope was associated with small values of wind direction steadiness and large values of duration. These parameters capture the physical torque effects of thousands of gust-lull cycles as well as the fact that, given the susceptibility of residential buildings to damage at roof corners and gables, the more the wind direction changes during a strong wind event, the greater the chance that a given wind direction will occur for which a structure is susceptible.

8. Conclusions

In order to achieve stable results, a very large simulation of ~100,000 years of activity is prescribed. It is expected that the model would be run once per year to take advantage of the latest historical data to assess average annual loss to residential properties due hurricane wind damage. The primary user will be the Department of Financial Services and homeowners in the state of Florida, although there are many other research uses for the model and it is expected that the model will undergo periodic enhancements to attempt to keep up with the state of the art. The model will reside at Florida International University's International Hurricane Research Center in Miami. Complete documentation of the model algorithms and code will be available for public examination. Given that there may be one Florida hurricane landfall per year, this large number of storms will be contained in our database. Each storm may effect as many as 40 zip codes so it is expected that the database could contain several million time series instances, as well as track, intensity, and landfall wind field information on each storm. The database could then be queried for details on simulated storms and probability distributions relevant to a given zip code or county in Florida. The model is scheduled for submission in 2004 to the State of Florida Commission on Hurricane Wind Loss Projection (Ref. [34]).

Acknowledgements

This research is supported by the State of Florida through a Department of Financial Services grant to the Florida International University International Hurricane Research Center. We thank the Department of Homeland Security (Federal Emergency Management Agency) and the National Institute for Building Sciences for their assistance with the roughness classifications.

Appendix: Hurricane Model Equations and Integration

1. Definitions

R = Radius of maximum surface wind speed, specified

c_t = storm translation speed, specified

c_{dir} = storm translation direction compass heading , specified

Δp = Central pressure deficit, specified

$p(r) = p_o + \Delta p e^{-\left(\frac{R_{\max}}{r}\right)^B}$ = sea level pressure

$B = 1.38 + 0.00184\Delta p - 0.00309R$ = Holland profile parameter

θ = Azimuthal coordinate, measured from north

$s = \frac{r}{R}$ = normalized radial coordinate

$v_g(s)$ = Gradient wind: $\frac{v_g^2}{r} + fv_g = \frac{1}{\rho}\frac{\partial p}{\partial r}$

$f = 2\Omega \sin\phi$ =Coriolis parameter

ϕ = latitude of storm center

$v_{o(s)}$ = normalized gradient wind (symmetric) = $v_{g(s)} / v_{gmax}$ where V_{gmax} is the maximum gradient wind in the radial profile

$\bar{f} = \frac{Rf}{V_{g\max}}$ = normalized Coriolis parameter

$v(s,\theta) = \frac{v}{v_g} =$ normalized storm-relative tangential wind component

$u(s,\theta) = \frac{u}{v_g} =$ normalized storm-relative radial wind component

/ /= friction coefficient= $\frac{RC_d}{h}$

h= mean boundary layer height

C_d = Drag Coefficient

$c = \frac{c_t}{v_{g\,\max}}$ = normalized translation speed

$g(s) = 2v_o(s)s^{-1} + \bar{f}$ (A1)

$d(s) = \dot{v}_o + v_o s^{-1} + \bar{f}$ (A2)

where a "dot" represents a derivative with respect to s, $g(s)$ and $d(s)$ depend only on V_0 and $\bar{f}$

$\zeta(s,\zeta) = v(s,\zeta) - v_o(s)$ = normalized departure from gradient balance

2. Equations of motion for a stationary storm

Substituting the terms from the definitions into (1) and (2) for a steady state, stationary storm (hence no azimuthal dependence: u = u(s) and / /= / /(s)) leads to the following normalized equations of motion:

$u\dot{u} - \zeta\left(g + \zeta s^{-1}\right) + \zeta uw = 0$ (A3)

$u\left(\zeta + \zeta s^{-1} + d\right) + \zeta\left(v_o + \zeta\right)w = 0$ (A4)

$w = \sqrt{u^2 + (vo + \zeta)^2}$ (A5)

w is the total normalized storm-relative wind vector.

3. Complete equations for a storm moving *northward* with translation speed c_t:

$u\partial_s u + s^{-1}\left(v_o + \zeta\right)\partial_\zeta u - \zeta\left(g + \zeta s^{-1}\right) + \zeta\left(uw + c\left(w - c\right)\sin\zeta\right) = 0$ (A6)

$u\partial_s \zeta + s^{-1}\left(vo + \zeta\right)\partial_\zeta \zeta + u\left(d + \zeta s^{-1}\right) + \zeta\left(\left(v_o + \zeta\right)w + c\left(w - c\right)\cos\zeta\right) = 0$ (A7)

$w = \sqrt{(u + c\sin\zeta)^2 + \left(\left(vo + \zeta\right) + c\cos\zeta\right)^2}$ (A8)

4. Solve Spoke equations

Let $\square = v_o + \square$ (A9)

$$u^* \partial_s u + \square u w^* \square \left(g + \square s^{\square 1}\right)^* \square + \left[s^{\square 1} \square \partial_\square u + \square\left(c\left(w \square c\right)\sin \square\right)\right]^* = 0 \quad \text{(A10)}$$

$$u^* \partial_s \square + \square\square w^* + \left(d + \square s^{\square 1}\right)^* u + \left[s^{\square 1} \square \partial_\square \square + \square\left(w v_o + c\left(w \square c\right)\cos \square\right)\right]^* = 0 \quad \text{(A11)}$$

These are linear in u and $\square$ if * terms are evaluated with fields from the previous iteration.

5. Solve Ring equations

$$\left(s^{\square 1}\square\right)^* \partial_\square u + \left(\partial_s u + \square w\right)^* u \square \left(g + s^{\square 1}\square\right)^* \square + \square\left(c\left(w \square c\right)\sin \square\right)^* = 0 \quad \text{(A12)}$$

$$\left(s^{\square 1}\square\right)^* \partial_\square \square + \left(\partial_s \square + s^{\square 1}\square + d\right)^* u + \square w^* \square + \square\left(v_o w + c\left(w \square c\right)\cos \square\right)^* = 0 \quad \text{(A13)}$$

These are linear in u and $\square$ if * terms are evaluated with fields from the previous iteration.

6. Substitute a linear combination of each solution back into the complete equations (Item 3 above) such that

$u = Au_s + Bu_r$ (A14)

and

$\square = A\square_s + B\square_r$ (A15)

7. Compute the residuals (or "non zeroness" of the solutions to the complete equations) at points in the core of the storm near the peak wind area and select the values for A and B that minimize the residuals throughout this region such that the value of J is as small as possible.

J = max (ABS (Res u) + ABS (Res$\square$)) (A16)

8. The sequence (Items 4-7) is repeated until the solution converges. Equations (14) and (15) are used to evaluate the * terms in items 4 and 5 for the next iteration.

9. Once the wind field is determined, it is rotated such that zero in the azimuthal coordinate matches the specified storm translation direction compass heading.

References

1. Russell, L. R., 1971: Probability distributions for hurricane effects. Journal of Waterways, Harbors, and Coastal Engineering Division, ASCE, 97, 139-154.

2. Landsea , C.W., R.A. Pielke, Jr, A.M. Mestas-Nunez, and J.A. Knaff, 1999: Atlantic basin hurricanes: Indices of climatic changes, *Climatic Change*,42 , 89-129.

3. Darling, R. W. R., 1991: Estimating probabilities of hurricane wind speeds using a large scale empirical model, Journal of Climate, 4, 1035-1046.

4. Rotunno, R. and K.A. Emanuel, 1987: An air-sea interaction theory for tropical cyclones, Part II. Part I. *J. Atmos. Sci.* ,42 , 1062-1071

5. Willoughby, H. E., and M. D. Shoreibah, 1982: Concentric eyewalls, secondary wind maxima, and the evolution of the hurricane vortex. J. Atmos. Sci., 39, 395-411.

6. Powell, M. D., and S. H. Houston, 1996: Hurricane Andrew's Landfall in South Florida. Part II: Surface Wind Fields and Potential Real-time Applications. Weather. Forecast., 11, 329-349.

7. Shay, L. K., G. J. Goni, and P. G. Black, 2000: Effects of a warm oceanic feature on Hurricane Opal. Mon. Wea. Rev., 125(5) ,1366-1383.

8. Miller, B. I., 1964: A study on the filling of Hurricane Donna (1960) over land. Mon. Wea. Rev., 92, 389-406

9. Powell, M. D., 1982: The transition of the Hurricane Frederic boundary layer wind field from the open Gulf of Mexico to landfall. *Mon. Wea. Rev*., 110, 1912-1932.

10. Vickery, P. J., and L. A. Twisdale, 1995: Wind field and filling models for hurricane wind speed predictions, Journal of Structural Engineering, 121, 1700-1709.

11. Ho, F. P., J. C. Su, K. L. Hanevich, R. J. Smith, and F. P. Richards, 1987: Hurricane climatiology for the Atlantic and Gulf coasts of the United States. NOAA Tech Memo NWS 38, NWS Silver Spring, MD.

12. Tuleya, R. E., M. A. Bender, and Y. Kurihara, 1984: A simulation study of the landfall of tropical cyclones using a movable nested-mesh model. *Mon. Wea. Rev.,* 112 , 124-136.

13. Kaplan, J. and M. DeMaria, 1995: A Simple Empirical Model for Predicting the Decay of Tropical Cyclone Winds After Landfall. J. App. Meteor., 34,

14. Ooyama, K. V., 1969: Numerical simulation of the life cycle of tropical cyclones. J. Atmos.

Sci., 26, 3-40.

15. Shapiro, L. 1983: The asymmetric boundary layer flow under a translating hurricane. J. Atmos. Sci., 40, 1984-1998.

16. Thompson, E. F., and V. J. Cardone, 1996: Practical modeling of hurricane surface wind fields, Journal of Waterways, Port, Coastal, and Ocean Engineering Division, ASCE, 122, 195-205.

17. Vickery, P. J., P. F. Skerjl, A. C. Steckley, and L. A. Twisdale, 2000a: A hurricane wind field model for use in simulations. Journal of Structural Engineering, 126, 1203-1222.

18. Vickery, P. J., P. F. Skerjl, , and L. A. Twisdale, 2000b: Simulation of hurricane risk in the United States using an empirical storm track modeling technique, Journal of Structural Engineering., 126, 1222-1237.

19. Kurihara, Y. M., M. A. Bender, R. E. Tuleya, and R. J. Ross, 1995: Improvements in the GFDL hurricane prediction system. Mon. Wea. Rev., 123, 2791-2801.

20. Holland, G. J., 1980: An analytic model of the wind and pressure profiles in hurricanes, Mon. Wea. Rev., 108, 1212-1218.

21. Dunion,J.P. , C.W.Landsea, and S.H.Houston (2003) "A re-analysis of the surface winds for Hurricane Donna of 1960" Accepted by Mon. Wea. Rev.

22. Willoughby, H. E. and E. Rahn, 2002:A new parametric model of hurrican wind profiles. 25th AMS COnference on Hurricanes and Tropical Meteorology, San Diego, 29 April - 3 May 2002.

23. Powell, M. D., P. J. Vickery, and T. Reinhold, 2003: Reduced drag coefficient for high wind speeds in tropical cyclones. Nature, 422, 279-283.

24. Large, W. G. and S. Pond, 1981: Open ocean momentum flux measurements in moderate to strong winds. *J. Phys. Oceanography*, 11, 324-336.

25. Moss, M. S. and S. L. Rosenthal, 1975: On the estimation of planetary boundary layer variables in mature hurricanes. Mon. Wea. Rev., 106, 841-849.

26. Powell, M.D., 1980: Evaluations of diagnostic marine boundary layer models applied to hurricanes. *Mon.Wea. Rev*., 108, 757-766.

27. Powell, M. D., S. H. Houston, and T. Reinhold, 1996: Hurricane Andrew's landfall in south Florida. Part I: Standardizing measurements for documentation of surface wind fields. *Wea.*

Forecasting., 11**,** 304-328.

28. Anctil, F. and M. Donelan, 1996: Air-water momentum flux observations over shoaling waves. J. Phys. Oceanogr., 26, 1344-1353.

29. Simiu, E., and R. H. Scanlan, 1996: Wind effects on structures: Fundamentals and applications to design. John WIley and Sons, NY, NY.

30. Peterson, E. W., 1969: Modification of mean flow and turbulent energy by a change in surface roughness under conditions of neutral stability. Quart. J. Roy. Meteor. Soc., 95, 561-575.

31. Schmidt, H. P. and T. R. Oke 1990: A model to estimate the source area contributing to turbulent exchange in the surface layer over patchy terrain. Quart. J. Roy. Meteor. Soc., 116, 965-988.

32. Vogelmann, J.E., S.M. Howard, L. Yang, C.R. Larson, B.K. Wylie, N. Van Driel, 2001. Completion of the 1990s National Land Cover Data Set for the Conterminous United States from Landsat Thematic Mapper Data and Ancillary Data Sources, Photogrammetric Engineering and Remote Sensing, 67:650-652.

33. Powell, M. D., S. H. Houston, and Ares, I. 1995: Real-time Damage Assessment in Hurricanes. 21st AMS Conference on Hurricanes and Tropical Meteorology , Miami, FL; April 24-28, 1995; Paper 12A.4 pp.500-502

34. Commission 2003: Report of Activities as of November 1, 2003. Florida Commission on Hurricane Loss Projection Methodology, Available from www.fsba.state.fl.us/methodology/meetings.asp

Figure Captions

1. Threat area map. All storms entering or developing within the threat area are considered for characteristics relating to formation, movement, and intensity.

2. Geographic distribution of probability of a storm entering or developing within the threat area.

3. Probability of a change in direction of storm motion to the left or right of the current motion as a function of the current storm heading (in degrees from north).

4. Polar coordinate ring and spoke system for solving equations of motion.

5. Horizontal distribution of mean boundary layer wind speed, relative to the moving storm for a simulation of Hurricane Georges. a) Ring solution, b) Spoke solution. Storm moving northward at 4.65 m/s. Horizontal coordinates are scaled by the radius of maximum wind, wind speed is scaled by the maximum gradient wind speed.

6. Same as Fig. 5 but for earth relative wind field resulting from optimal combination of ring and spoke solutions to best solve the scaled versions of eauations (1) and (2).

7. Comparisons of model surface wind field to observation based analysis of Hurricane Andrew (1992). Wind fields represent maximum sustained (1 min) wind speeds in knots. To convert to meters per second multiply by 2.23.

8. Distribution of aerodynamic roughness for the State of Florida determined from multi-resolution land-use land-cover classifications.

*Corresponding author :

Dr. Mark D. Powell
4301 Rickenbacker Cswy.
Miami FL 33149
USA

E-mail: Mark.Powell@noaa.gov

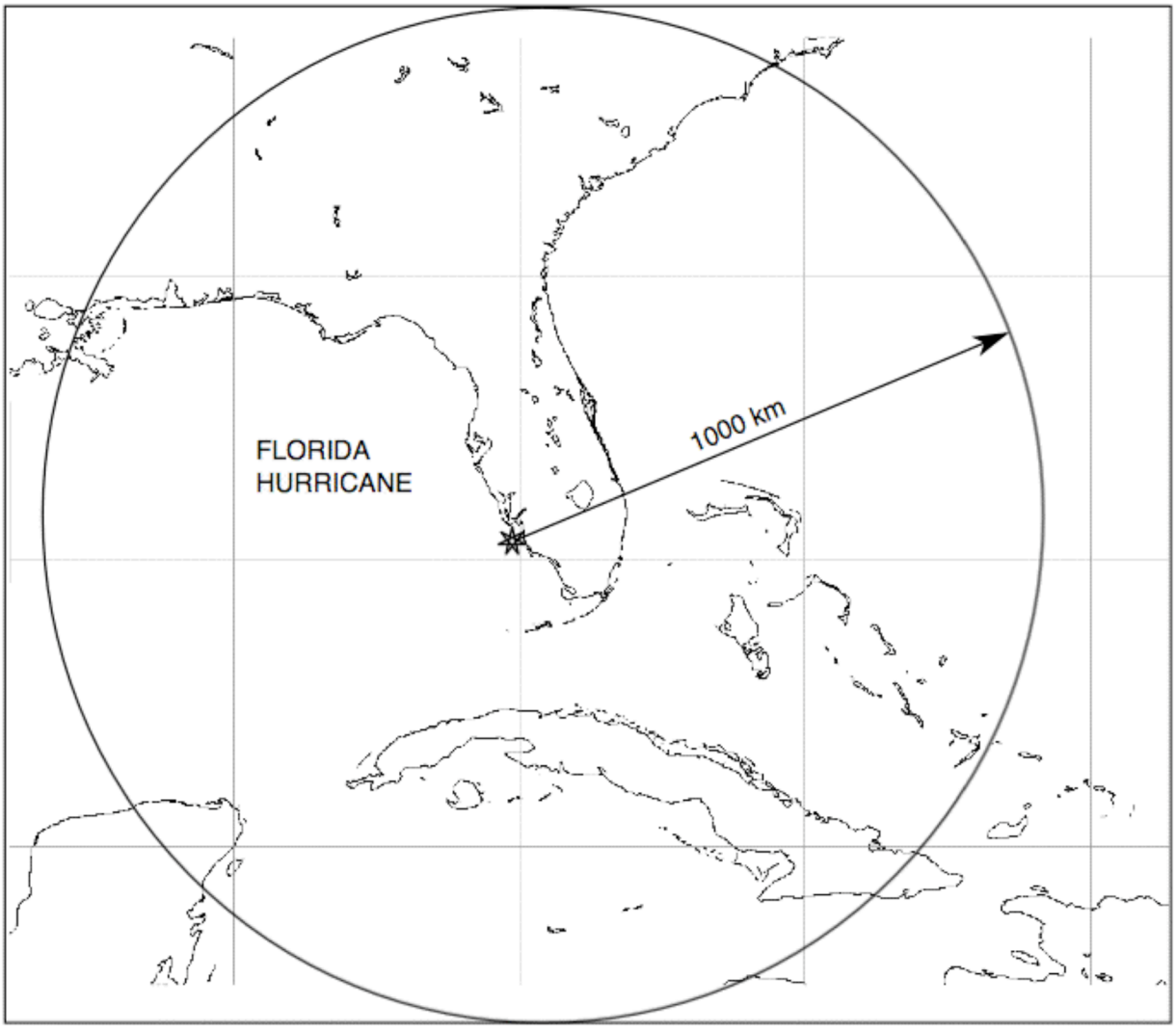

Figure 1. Threat area map. All storms entering or developing within the threat area are considered for characteristics relating to formation, movement, and intensity.

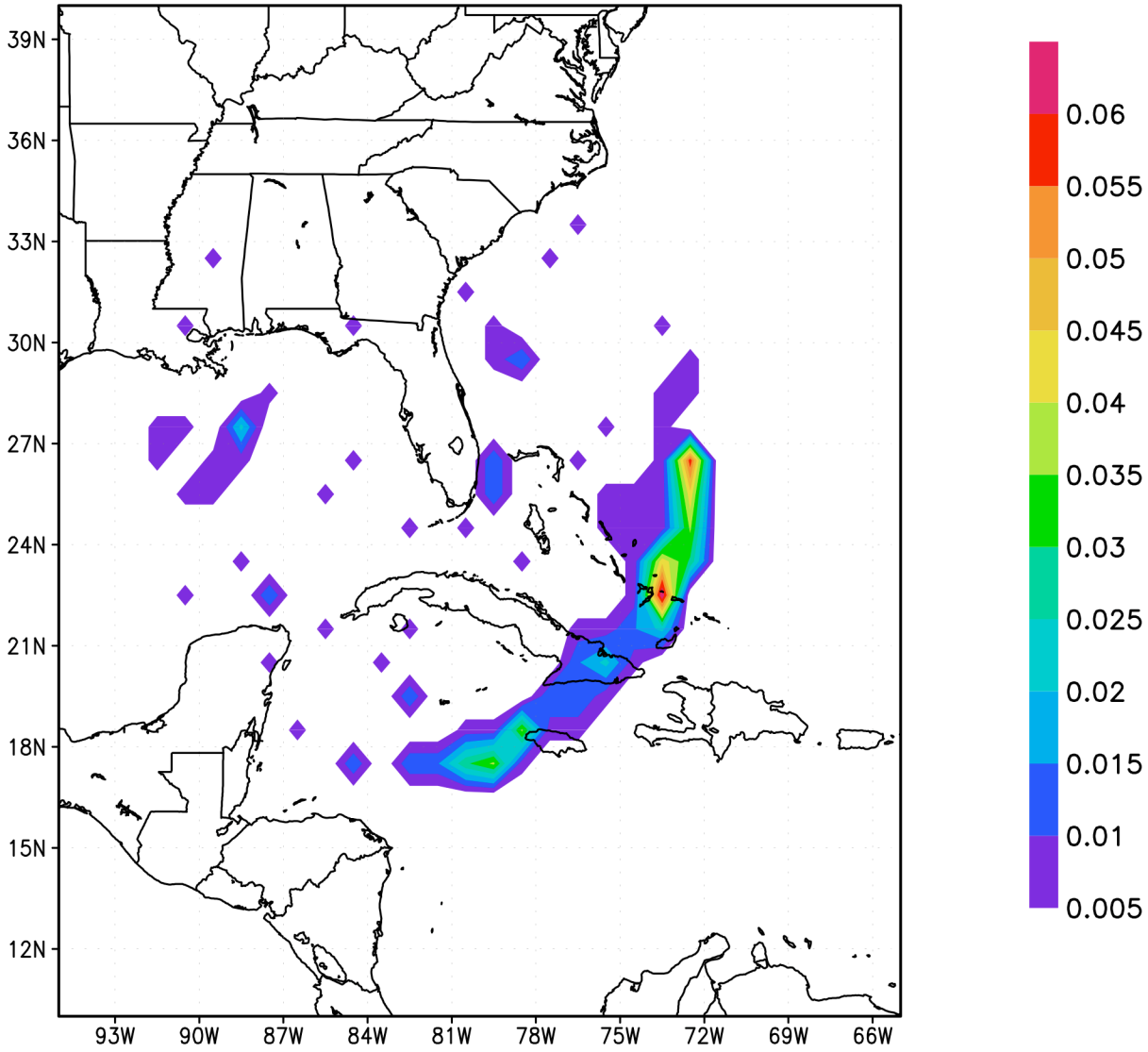

2. Geographic distribution of probability of a storm entering or developing within the threat area.

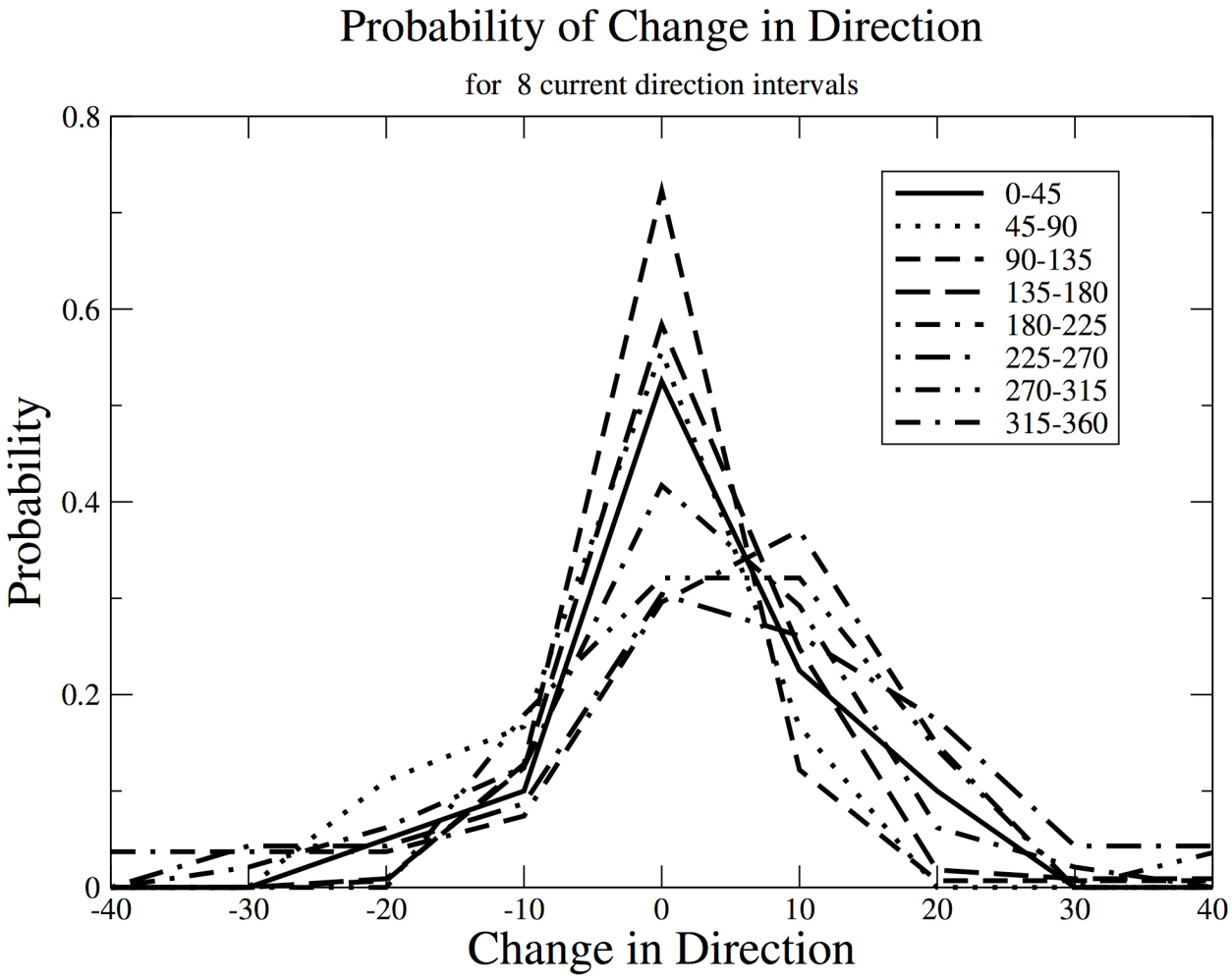

3. Probability of a change in direction of storm motion to the left or right of the current motion as a function of the current storm heading (in degrees from north).

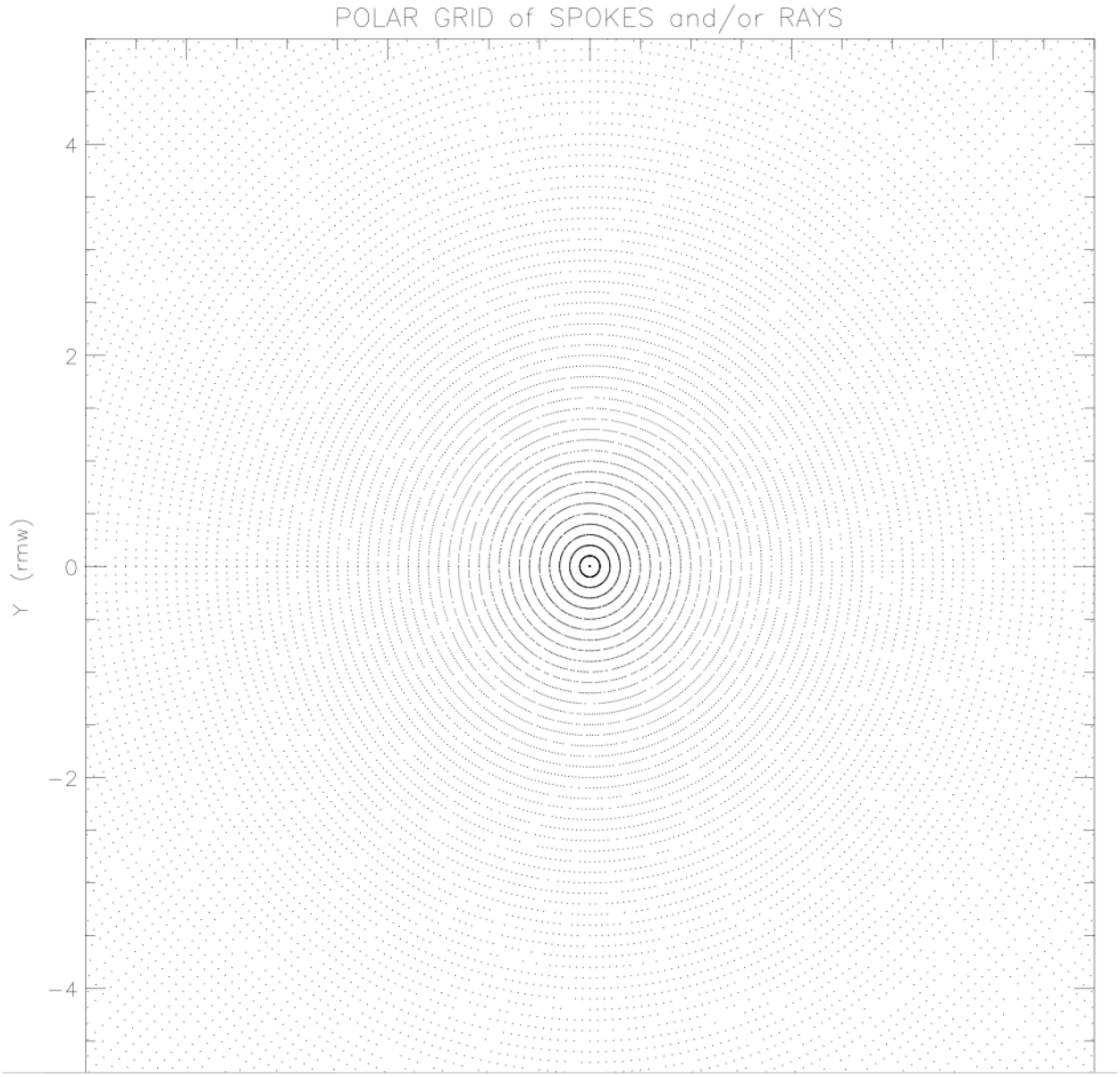

4. Polar coordinate ring and spoke system for solving equations of motion.

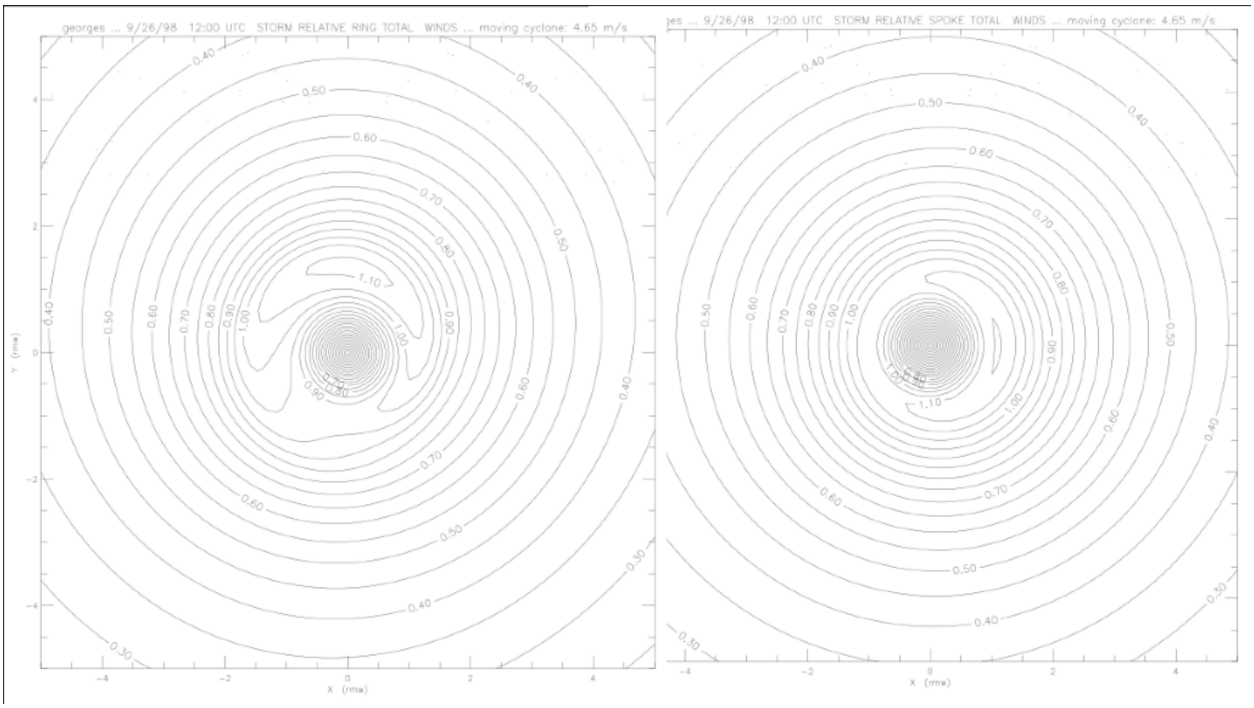

5. Horizontal distribution of mean boundary layer wind speed, relative to the moving storm for a simulation of Hurricane Georges. a) Ring solution, b) Spoke solution. Storm moving northward at 4.65 m/s. Horizontal coordinates are scaled by the radius of maximum wind, wind speed is scaled by the maximum gradient wind speed.

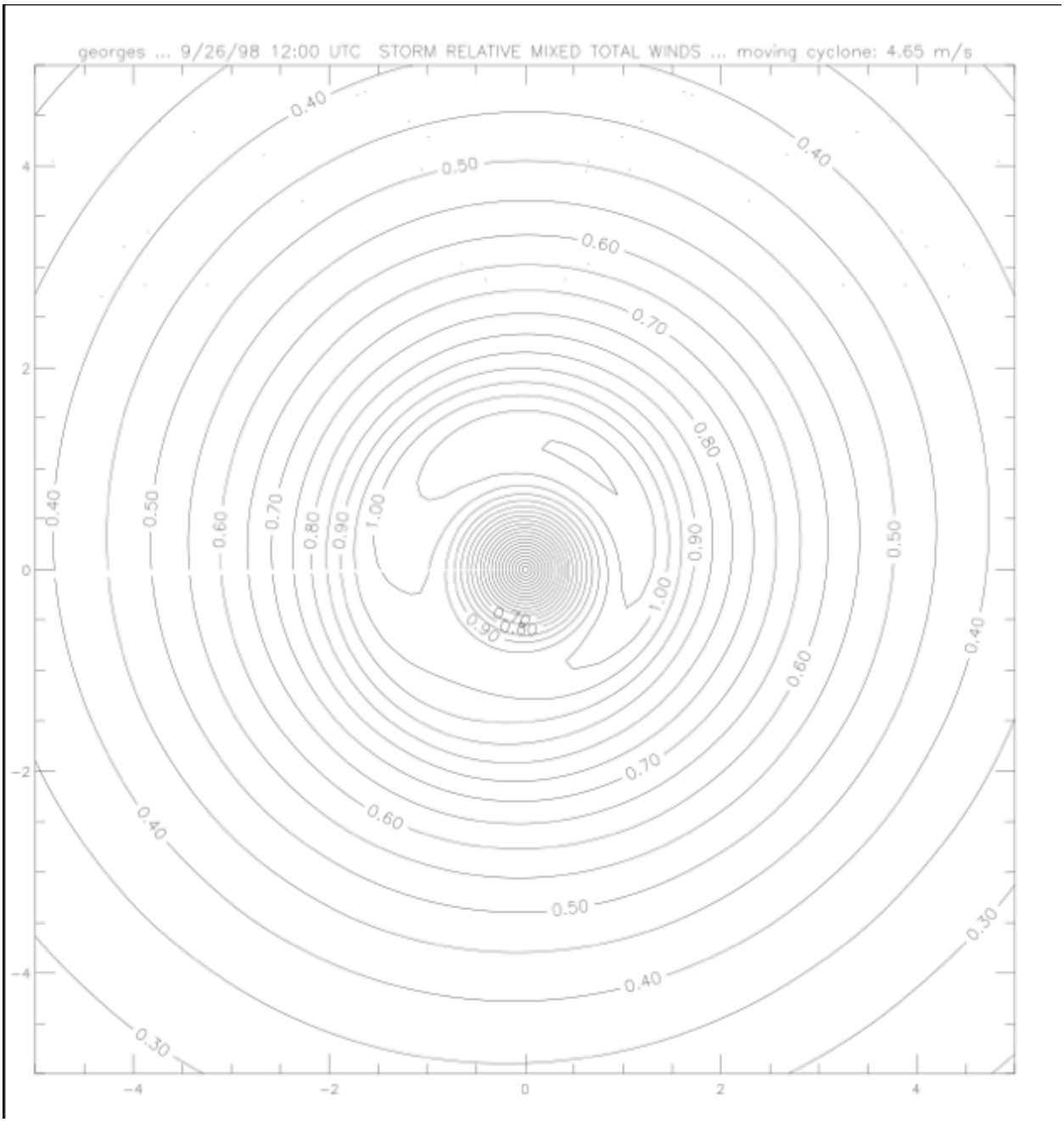

6. Same as Fig. 5 but wind field resulting from optimal combination of ring and spoke solutions to best solve the scaled versions of equations (1) and (2).

Model

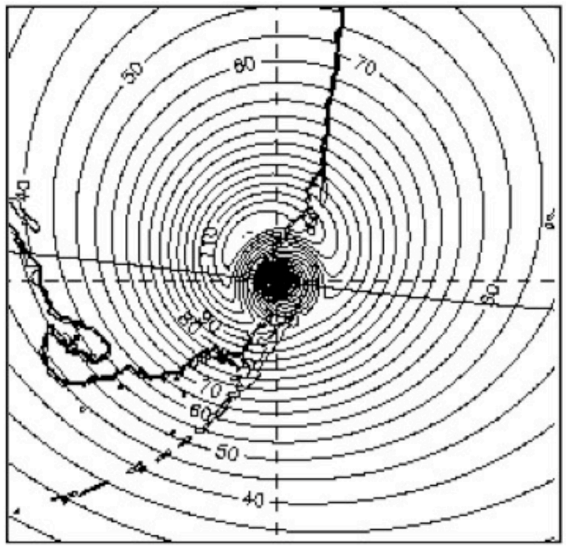

Observed

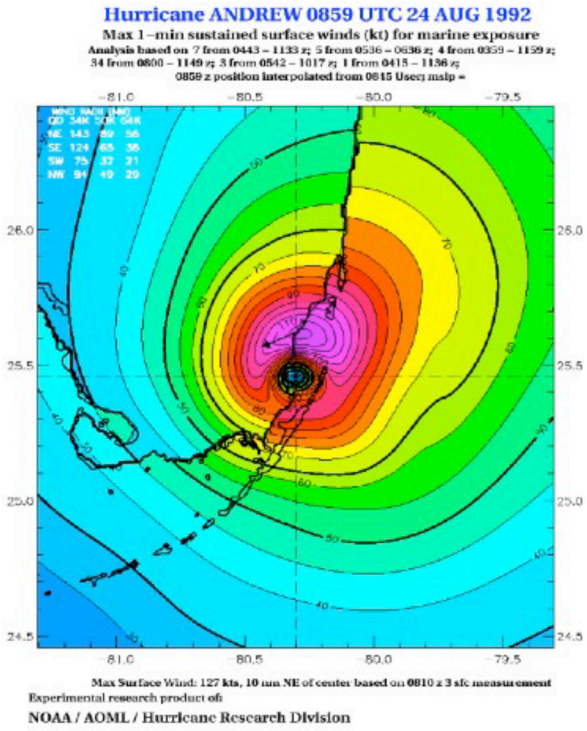

7. Comparisons of model surface wind field to observation based analysis of Hurricane Andrew (1992). Wind fields represent maximum sustained (1 min) wind speeds in knots. To convert to meters per second multiply by 2.23.

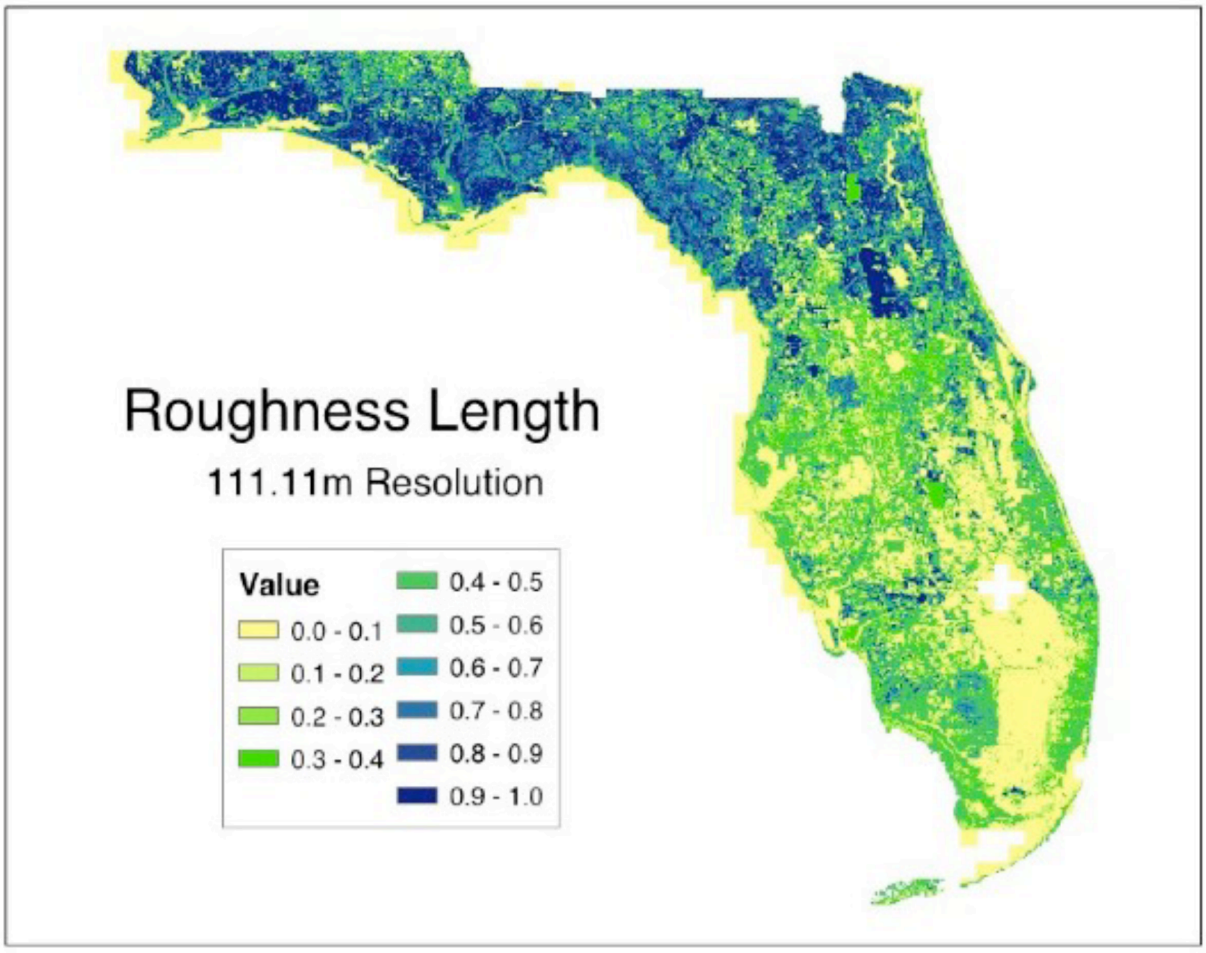

7. Distribution of aerodynamic roughness for the State of Florida determined from multi-resolution land-use land-cover classifications.